Solid-State NMR of Aromatic Polyamides

S. A. Curran,* C. P. LaClair, and S. M. Aharoni

Research and Technology, Allied Signal, Inc., Morristown, New Jersey 07962

Received December 19, 1990; Revised Manuscript Received June 26, 1991

ABSTRACT: We have investigated the solid-state ^{13}C NMR behavior of a series of dry and swollen rigid polyamides. The dry polymers exhibit rigid, glassy polymer characteristics, but results for the swollen gels are quite surprising. The relaxation behavior for swollen polymers is quite sensitive to temperature. The 30% linear polyamide solution undergoes a transition from a physical gel to a liquid crystal in the 65–70 °C range accompanied by dramatic changes in the chemical shift anisotropy (CSA) and relaxation rates at the phase transition. The swollen gels of the branched polymers do not become liquid crystalline and we did not observe dramatic changes in CSA, but they do undergo transitions, with marked relaxation rate changes in the 60–80 °C range. The activation energies for relaxation were calculated from an Arrhenius plot. The $T_{1\rho C}$ temperature dependence, particularly for swollen polymers, indicates that hydrogen-bond breaking and anti/syn interconversion is a major relaxation pathway. CP/MAS results support the formation of crystallosolvates in both linear and network polymers. We have obtained the NMR spectrum of the solvent (*N,N*-dimethylacetamide) in the crystallosolvates and observe an unexpectedly strong cross-polarization signal for DMAc and DMAc-d_9 in 30% polymer solutions. In effect, a fraction of the DMAc solvent enters a solid complex between solvent and polymer, with very slow solvent exchange.

Introduction

A large family of highly branched rigid aromatic polyamide networks and gels as recently been prepared in solution by a one-step polycondensation reaction.[1-5] They are characterized by stiff segments of average length l_0 covalently connected at both ends by rigid polyfunctional branch points. In the pregel stage, the growing polymeric species were found to obey the fractal model and will therefore be called fractal polymers (FPs). By withdrawing aliquots from the reaction mixture at incremental times and then precipitating and purifying the FPs, we obtained a series of FPs of identical structure but of increasing FP molecular weight and size. After characterization, the FPs were again placed in the reaction medium, this time in the absence of any monomeric or oligomeric species, and the polycondensation reaction continued past the gel point, producing sturdy stiff gels.

These FPs and their networks are amorphous in nature,[3-5] with randomly oriented stiff segments. Because of this, the number of intersegmental hydrogen bonds (H-bonds) is greatly reduced relative to their number in linear polyamides of comparable structure.[4,6,7] In the gelled network or solvent-swollen FPs the number of intersegmental H-bonds is further reduced in favor of segment–solvent H-bonds. The polymers analyzed in this study are highly branched FPs and their network progenies, characterized by stiff segments with an average length of 38.5 Å connected to one another by rigid trifunctional branch points. A typical fragment is 1 (Chart I).

The nitro substitution on the middle aromatic ring in the stiff segment greatly increases the solubility of the pregel FPs in the reaction mixture and in the excellent solvents *N,N*-dimethylacetamide (DMAc) and DMAc/LiCl.[1,8] As a result, the "as-prepared" and the DMAc-equilibrated networks are optically isotropic and blemishless. For comparison, a linear analogue of the FPs was prepared and studied. A typical repeating unit is 2 (Chart I). This linear polymer exhibits lyotropic liquid crystallinity, and the presence of a nitro group on every third ring has only minimal effects on the linearity of the stiff chain.[8] At sufficiently high concentration and low temperature this polymer forms a thermoreversible gel. This is a physical agglomeration phenomenon, while the other samples studied are covalently bound gels.

It was previously demonstrated by one of us that stiff polyamide segments unconstrained from free motion on at least one end may preferentially deform and bend by a single anti/syn or syn/anti interconversion of an amide group relative to its adjacent aromatic rings.[6] When built into a network or a fractal polymer with both ends constrained from torsional motions, the stiff segments can bend by two anti/syn or syn/anti interconversions per segment. Such deformations occur through rotations around the ring-to-carbonyl bond and to a lesser extent around the ring-to-nitrogen bond.[10] They require relatively low activation energies, similar in magnitude to those associated with ring flipping.[11]

The fractal polymers and rigid networks have previously been studied by several techniques.[3-6] In particular, solid-state ^{13}C NMR has been reported on these [4-7] and similar [12] polymers. Cross-polarization magic angle spinning (CP/MAS) was used to study the ^{13}C NMR chemical shifts of the FPs and networks.[6] While analysis of chemical shifts proved valuable, a potentially even more potent use of solid-state NMR for these polymers is the study of molecular motions. NMR relaxation behavior provides details on molecular motion of the polymer chains,[13-16] where the motional frequency studied is determined by the choice of experiment.

In this case we chose to measure $T_{1\rho C}$ as a function of temperature. The high resolution and sensitivity of CP/MAS ^{13}C NMR allow us to monitor each type of carbon in the polyamide. In addition, the relationship between physical properties and the kilohertz frequency motions measured via $T_{1\rho C}$ is well established.[14,17-22] There is one major complication in the use of $T_{1\rho C}$ to characterize molecular motions. Care must be taken in quantitatively interpreting relaxation rates since they are known to depend on fluctuations of the ^1H homonuclear dipolar coupling as well as molecular motions, particularly in rigid polymers.[19-24] This complicates our interpretation for the dry polyamides so that we cannot draw direct conclusions about the degree of mobility in the dry polymers simply from the magnitude of the relaxation rate, but our evidence in these systems shows that relaxation is primarily via kilohertz motions rather than dipolar fluctuations. Therefore, qualitative observations of phase transitions and temperature dependence in the dry samples are still valid. In

0024-9297/91/2224-5903$02.50/0

Chart I

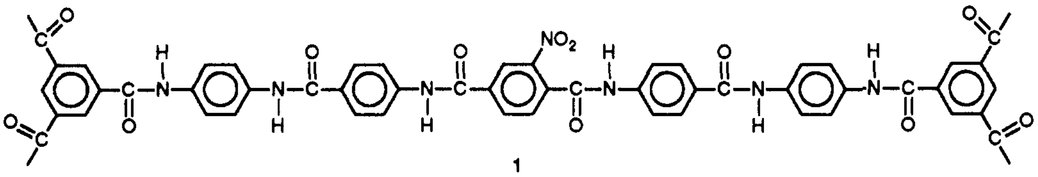

1

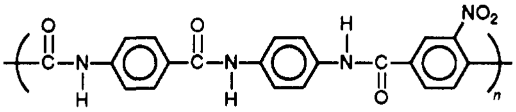

2

the case of swollen networks, carbon–proton interactions do not appear to be a serious problem, and the interpretation is similar to that for glassy polymers, so that interpretation is straightforward.

$T_{1\rho C}$ is usually reported as an average relaxation rate: $\langle T_{1\rho C}\rangle$.[14,20] In this report we detail a study of $\langle T_{1\rho C}\rangle$ (determined with spin-lock times between 50 and 900 μs) dependence on temperature for rigid, linear, branched FP and network polyamides across a wide temperature range. They were analyzed both in a dry state and as swollen networks, 30 wt % in DMAc/5% LiCl. The most interesting results were in the swollen polymers.

The highly concentrated linear polymer solution exhibits a dramatic change in chemical shift anisotropy (CSA) at elevated temperature, which we interpret as a thermoreversible physical gel to liquid crystal phase transition. The branched FPs and networks are rigid and remained randomly oriented throughout the temperature range studied. We observe limited mobility below a transition with the onset of amide group reorientation above the transition. The nature of this reorientation is discussed below.

Experimental Section

The preparation and characteristics of the investigated samples have been described previously.[5,8] The linear segments are poly(*p*-benzanilide–nitroterephthalamide), and they have rigid trifunctional branch points as shown in structure 1. Specific details on the samples are given with the discussion of their NMR behavior.

The DMAc/LiCl and DMAc-d_9/LiCl solutions were prepared by placing 5 wt % LiCl (reagent grade) in DMAc or DMAc-d_9 and gently heating. Swollen systems containing 30 wt % polymer were prepared by adding the desired quantity of solvent to dry polymer and heating at 60 °C overnight.

A typical ^{13}C CP/MAS spectrum for a dry rigid network (N74D as described below) is given in Figure 1. All NMR spectra were acquired on a Chemagnetics CMX-300 solid-state NMR spectrometer. Proton 90° pulses were 5 μs. CP contact times were 1.0 ms with 50-kHz ^{1}H and ^{13}C spin lock for the results reported here. The proton decoupler strengths were 80 and 100 kHz for swollen and dry polymers, respectively. The 50-kHz carbon spin lock hold times after CP varied between 0.05 and 0.9 ms.

Cycle times were set to 2 s to allow complete proton spin–lattice relaxation. All samples were placed directly in a zirconia rotor and inserted in the Chemagnetics double-air-bearing MAS probe (pencil probe). Spinning speeds were 3–4 kHz. Initial experiments with an earlier probe design required added KBr with the swollen gels for proper balance. The pencil probe did not need KBr to balance the rotors, so it was omitted. The magic angle was set within 0.1° prior to analysis with a reference sample of KBr, using the ^{79}Br sideband technique.[25]

Results and Discussion

$\langle T_{1\rho C}\rangle$ relaxation rates for the dry and swollen polymers show a strong temperature dependence. We know that $\langle T_{1\rho C}\rangle$ depends on dipolar fluctuations in combination with molecular motions. We have made no attempt to quantitatively separate the two effects in these stiff amorphous polymers. We did investigate the room temperature H_{1C} dependence of $\langle T_{1\rho C}\rangle$ for the linear sample and one FP, both in the dry state. With a 50-kHz carbon spin lock we obtained $\langle T_{1\rho C}\rangle$'s of 66 and 46 ms respectively for the linear polymer and FP74D discussed below. Using a 90-kHz spin lock, the measured $\langle T_{1\rho C}\rangle$ values were 143 ms for the linear polymer and 100 ms for the FP. The remainder of the experiments were done using a 50-kHz spin lock to avoid prove arcing, which was a particular problem in the swollen samples. The relatively weak dependence of $\langle T_{1\rho C}\rangle$ on H_{1C} is good evidence that we are indeed monitoring relaxations primarily related to molecular motion rather than dipolar fluctuations. We therefore expect the FP's and network temperature dependence will show whether the chains are undergoing correlated motions or if the amide group and aromatic ring motions are decoupled from each other. All the FP's are quite similar, implying that they also will relax via kilohertz motions. Since swelling will increase chain motions, we can safely assume that the dominant relaxation mechanism for swollen polymers is also via kilohertz molecular motions. Thus, we can directly relate molecular motions to relaxation rates.

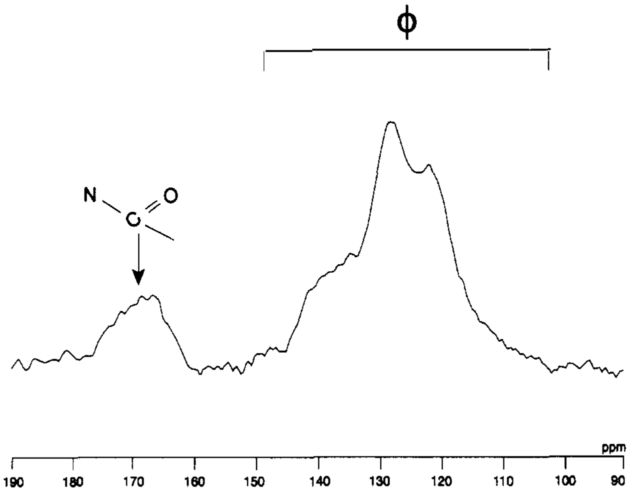

Figure 1. Typical solid-state CP/MAS ^{13}C spectrum of dry network.

Linear Polymer. The dry linear polymer, labeled L51D, had a weight-average molecular weight (M_w) of 12 700 and intrinsic viscosity of $[\eta] = 0.83$ dL/g. It shows a transition in the 55–65 °C range, as seen in Figure 2. While the relaxation rates are different for each type of carbon, the slopes of the $\langle T_{1\rho C}\rangle$ versus temperature curve are the same for temperatures between 25 and 55 °C. This indicates that the relaxation mechanism and its activation energy (E_a) are probably the same for all types of carbon in this temperature range.

There is a step change in all curves between 55 and 65 °C, indicating a change in relaxation mechanism. How-

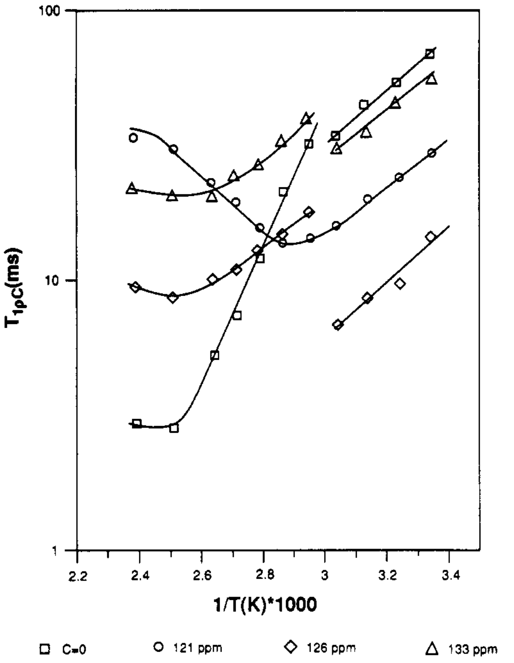

Figure 2. $\langle T_{1\rho C}\rangle$ temperature dependence for dry linear poly(*p*-benzanilide–nitroterephthalamide) (M_w = 12 700).

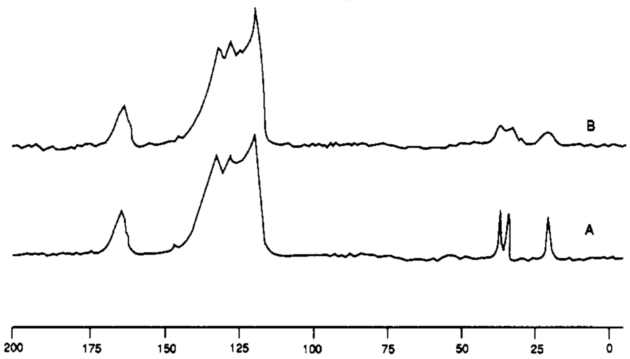

Figure 3. ^{13}C CP/MAS spectrum for linear polymer swollen in (A) DMAc/LiCl and (B) DMAC-d_9/LiCl.

ever, the aromatic ring carbons exhibit the same slope in the curve and therefore the same E_a for relaxation above and below this transition. Above the transition temperature, the slope of the curve for the amide carbonyl is steeper than that of the other carbons in the chain, consistent with faster reorientation of the carbonyls relative to the aromatic rings. While absolute relaxation rates may depend on dipolar fluctuations as well as molecular motion in this dry rigid polymer, clearly the relaxations of the carbonyl are drastically different and decoupled from those of the rings at elevated temperature.

There are a number of interesting effects observed in the 30% linear polymer solution. One intriguing observation is a strong signal from the DMAc solvent in a CP experiment (Figure 3A). Typical liquids do not give CP signals because CP requires a strong static H–C dipole for polarization transfer,[26,27] and freely tumbling liquids average dipolar interactions. The appearance of the DMAc signal in the spectrum therefore indicates highly restricted solvent mobility. These are two possible reasons for restricted mobility: adsorbed solvent could simply be trapped in the polymer network or we could be forming a solvent–polymer complex which makes the solvent essentially a solid.

We used DMAc-d_9 to discriminate between these mechanisms. Since CP depends on a strong static H–C dipolar coupling,[26,27] we expect no signal from deuterated solvent which is simply trapped in the polymer matrix. On the other hand, a complex should bring the solvent and polymer into intimate contact and allow cross polarization from the polymer protons to the solvent carbons. There is a strong solvent CP signal even in the DMAc-d_9 case, consistent with complexation as shown in Figure 3B.

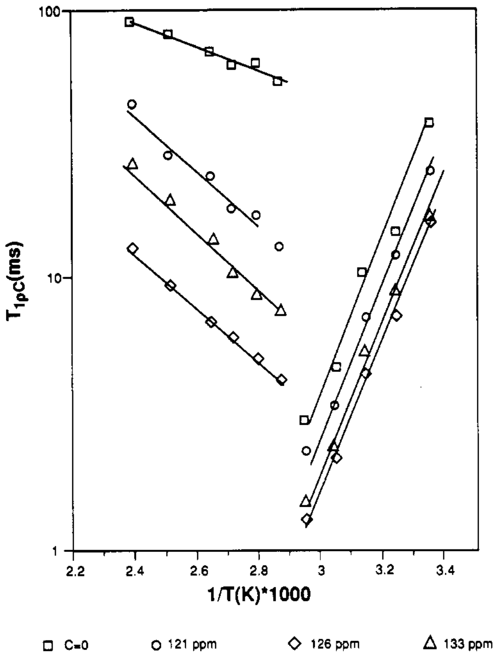

Figure 4. $\langle T_{1\rho C}\rangle$ temperature dependence for 30% linear polymer in DMAc/LiCl.

Similar systems have been reported to form "crystallosolvates"[28-30] where the solvent precipitates as a solid on the surface of the polymer. In the case of stiff zigzag polyamides, it was previously shown by a combination of light scattering and solution studies that "the polymer chains are encased in a dynamic sheath of solvent molecules, the thickness of which is about two to three molecules thick".[7] This type of structure is consistent with our observation on these rigid polyamides. It should be recalled that the concentrated solution contains 30 wt % polymer, which translates to only about 3.3 solvent molecules for each amide group along the segment or linear chain.

Note also the line width for the solvent in the polymer–DMAc-d_9 complex (Figure 3B). The solvent lines are significantly broader than for the protonated solvent. The additional line broadening is probably caused by strong ^{13}C–^{2}H coupling in the solid state. It may be due to *J* coupling, since we do not decouple ^{2}H, or it may be an effect of the deuterium quadrupole. We have not investigated this effect any further.

As with the dry polymer, the concentrated linear polymer solution exhibits a transition. In this case it is observed at 75 °C. Below this temperature the slope of the relaxation rate curves are the same for all carbons; see Figure 4. There is a step change in relaxation rates at the transition temperature and relaxation times begin to rise with temperature. However, the energy of activation for relaxation of the aromatic carbons does not change. As in the dry-polymer case, the $\langle T_{1\rho C}\rangle$ temperature dependence of the carbonyl group is quite different from that of the aromatic rings, indicating a decoupling of the amide relaxation from the ring relaxation. The activation energies below and above the transition temperatures of all samples studied were calculated from an Arrhenius plot and are listed in Table I.

Table I

sample	transition temp (T/°C)	E_a/(kcal mol^{-1})			
		low temp[a]		high temp[a]	
		C=O	Ar	C=O	Ar
linear L51D					
dry	55	4.3	4.2	14.0	4.2
swollen	75	13.4	13.0	2.3	5.5
large FP1 (F72A)					
dry	85	6.9	2.8	10.4	4.6
swollen	55	0.4	14.0	0.5	3.4
network 1 (N74D)					
dry	55-65	10.8	2.7	8.8	2.9
swollen	55	1.2	14.0	3.8	4.5
small FP2 (F74B)					
dry	85	7.1	1.8	7.9	4.0
swollen	55	0.5	14.0	1.9	4.6
network 2 (N74E)					
dry	75	19.7	9.2	8.2	7.1
swollen	75	2.0	12.8	7.9	7.7

[a] "Low temp" and "high temp" refer to E_a below and above the transition.

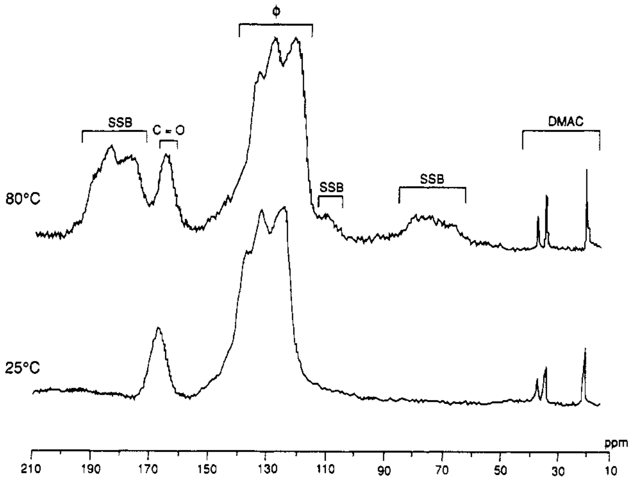

Figure 5. Development of spinning sidebands for 30% linear polymer in DMAc/LiCl at the transition temperature.

One additional interesting observation is the development of pronounced spinning sidebands in the spectrum at the transition temperature (Figure 5). Spinning sidebands are minimal at room temperature before heating, and, on cooling, sideband intensity slowly decreases with time and disappears when the sample is completely cooled to room temperature. At the transition temperature, the low-field spinning sideband in particular becomes large relative to the isotropic peak, consistent with a highly anisotropic sample. The large sidebands persist even at elevated temperature. These results indicate formation of physically anisotropic structure at the transition. On cooling, the anisotropy decreases slowly, until an isotropic structure is again obtained.

We attribute this effect to formation of a stable liquid crystalline phase in the very concentrated linear polymer solution at 75 °C. It has previously been demonstrated that linear stiff poly(p-benzanilide–nitroterephthalamides) (PBNT) such as L51D form liquid crystalline polymers,[8] so it is not surprising that we should observe such anisotropy. We believe the appearance of liquid crystallinity only above ca. 75 °C reflects the room temperature tendency of the PBNT family to form reversible gels when present at very high concentrations in DMAc/LiCl. We have made no attempt to measure the full temperature range where this anisotropic phase is stable but we observe this type of behavior up to the maximum temperature measured, 150 °C. We have not investigated whether magnetic field effects from the instrument or stress from MAS affect the development of liquid crystallinity.

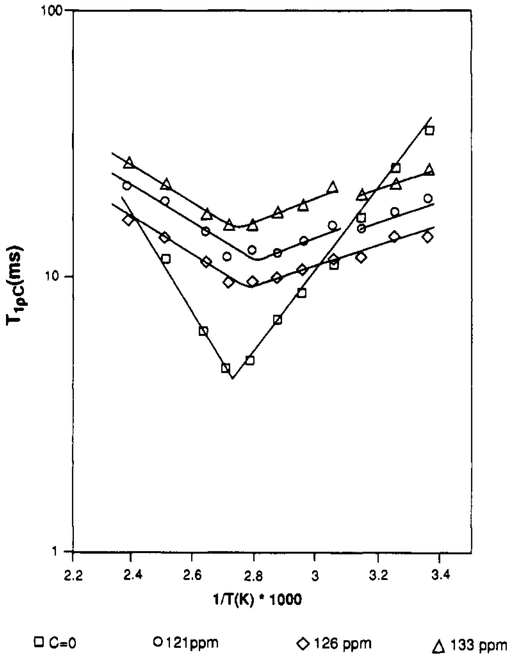

Figure 6. $\langle T_{1\rho C}\rangle$ temperature dependence for dry large FP F72A (poly(p-benzanilide–nitroterephthalamide)) with rigid trifunctional branch points (M_w = 320 000, M_n = 40 000).

Network Polymers. Large FP1. Sample F72A is a large FP with M_w = 320 000, M_n 40 000, hydrodynamic radius R_H = 180 Å, and $[\eta]$ = 1.09 dL/g. As with the dry linear polymer, the resonances of the dry FP sharpen slightly with increasing temperature and we observe signifnicant relaxation rate effects. The $\langle T_{1\rho C}\rangle$ temperature dependence is quite pronounced in the dry fractal polymer, as shown in Figure 6, but it is drastically different from the linear polymer response. The carbonyl relaxation in the FP is already decoupled from the ring relaxations at room temperature and remains decoupled throughout the temperature range investigated.

The curves show a change in slope, i.e., a change in the relaxation mechanism, at approximately 90 °C. The curves are somewhat deceptive. On first inspection, we seem to be observing a classical $T_{1\rho}$ minimum, with all the curves showing a minimum at approximately 90 °C. However, closer examination of the curves reveals different slopes above and below the minimum. Thus we are observing a change in relaxation mechanism rather than a simple correlation time minimum. The activation energy calculated from these slopes (Table I) is consistent with syn/anti and anti/syn interconversions of whole amide groups.[6,10] These interconversions have, however, activation energies identical with those of ring flips[11] since the rotational motions in both must surpass the *same* energy barriers. The calculated E_a increases above the transition temperature, consistent with introduction of a new relaxation mechanism, but there is still insufficient energy to provide for amide trans/cis isomerization.[6] We conclude that we have probably introduced new anti/syn and syn/anti interconversions which were excluded at low temperature.

The swollen FP's relaxation behavior parallels that of the linear polymer, but we see no development of large spinning sidebands at elevated temperature. This is as expected if the sideband effect in the linear case is from liquid crystallinity. Highly branched FPs do not form

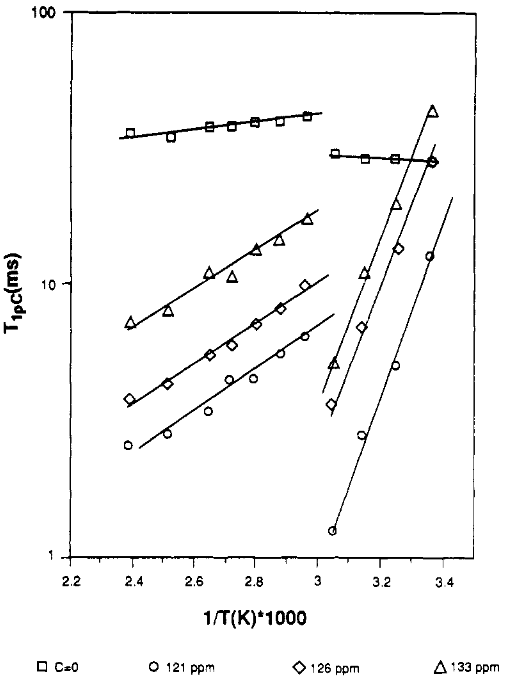

Figure 7. $\langle T_{1\rho C} \rangle$ temperature dependence for 30% large FP (F72A) in DMAc/LiCl.

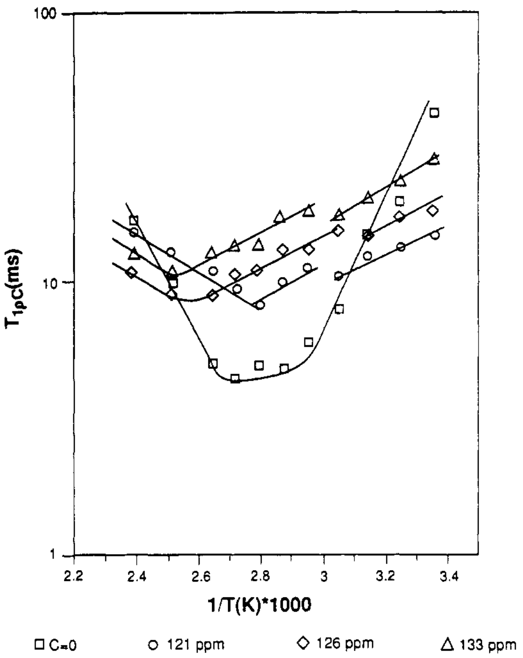

Figure 8. $\langle T_{1\rho C} \rangle$ temperature dependence for dry N74D, the network progeny of large FP (F72A).

liquid crystalline phases[4] and therefore should not show strong physical anisotropies.

The swollen FP does show a strong $\langle T_{1\rho C} \rangle$ temperature dependence; see Figure 7. Again the carbonyl relaxation is decoupled from the aromatic rings, and there is a step change in relaxation rates at 55 °C. Above the transition temperature the slopes of all the curves change dramatically. The ring carbons share the same temperature dependence at all temperatures, i.e., the same E_a for relaxation, while E_a for relaxation of the carbonyl is substantially lower. This is similar to the effect observed in the linear polymer, but much more pronounced. A direct comparison of E_a calculated for both dry and swollen samples gives lower activation energies in the branched FPs than for the linear polymer. Thus, despite sharing the same chemical structure, the stiff short segments between branch points have different mobilities than the long linear polyamides, at least in the kilohertz frequency range. Otherwise, relaxation behavior of the stiff segments between branch points should be identical with that of the linear rigid polymer.

We believe that the higher activation energies of the linear polyamide are an indirect reflection of the high level of cooperativity present in the dry and solvated linear polymer. This cooperative behavior, brought about through strongly H-bonded solvation leading to thermoreversible gel at low temperature and lyotropic liquid crystallinity at higher temperatures, is absent in the fractal polymers and their network progenies. The reason for the different behavior is not clearly understood, but we believe it reflects the fact that in the FPs and gelled networks the stiff segments are randomly oriented and constrained by their rigid branch points from reorienting to obtain a cooperative system. Naturally, such restrictions do not exist in the case of the rigid linear polyamides which can move and produce a cooperative system.

Network 1. Sample N74D is a network prepared from the large fractal polyamide F72A. Again there is a strong temperature dependence for relaxation rates (Figure 8). We observe a transition in the dry polymer at 55 °C, which is substantially lower than the transition temperature of the original FP. A comparison of E_a below and above the transition for the dry FP and dry network progeny shows interesting results. The activation energy at low temperatures is lower for the FP, while the situation is reversed above the transition temperature. While one might expect a network to be more rigid than the FP at room temperature, the apparently lower rigidity at elevated temperatures is surprising. It may well be the case that the network has a significantly different spectral distribution of homonuclear proton fluctuations, so that the results do not depend on molecular motions, but one would not expect such a strong temperature dependence in that case. The results are more consistent with the fact that even in large FPs a significant fraction of the segments are not constrained at both ends, allowing easier anti/syn interconversion.

The swollen gel shows quite reasonable results; see Figure 9. There is a transition in the 55–60 °C range. Relaxation of the aromatic ring shows significantly lower E_a above 60 °C. The observed aromatic ring relaxation activation energies are essentially the same as those of the FPs. The carbonyl group activation energies above and below the transition are in a reasonable range for syn/anti interconversion, but the E_a's are consistently higher than for the FP. These results indicate again that the primary relaxation mechanism is anti/syn interconversions and not anti/cis isomerization. The relatively low E_a values for the relaxation of the carbonyl carbons in the swollen N74D network reflects, we believe, the fact that in the presence of solvent the syn/anti interconversions tend to relax the entire network and the resultant total activation energy is smaller than the activation energy for rotation around each ring to carbonyl bond.

Small FP2. The second fractal polymer investigated (F74B) had the same composition as the large FP, but of a much smaller size: $M_w = 24\,000$, $M_n = 8000$, $R_H = 27.7$ Å, and $[\eta] = 0.39$ dL/g. The relaxation time versus temperature curve for the dry fractal in Figure 10 again shows correlated motions for the ring carbons, with the carbonyl decoupled from the rings, experiencing higher energy motions. The apparent minimum is not a classical $T_{1\rho C}$ minimum but a transition since the slope of the curve, and therefore E_a, changes as shown in Table I.

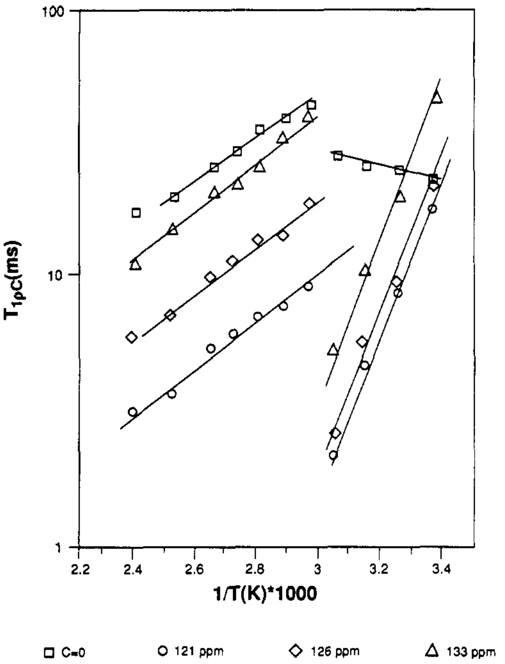

Figure 9. $\langle T_{1\rho C}\rangle$ temperature dependence for 30% N74D, the network progeny of large FP (F72A) in DMAc/LiCl.

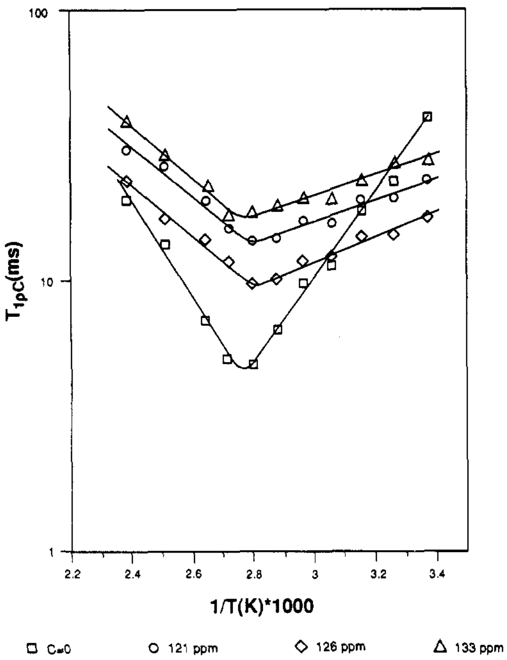

Figure 10. $\langle T_{1\rho C}\rangle$ temperature dependence for dry small FP F74B, with the same composition as the FP in Figure 6 and the same distance between branch points but with M_w = 24 000 and M_n = 8000.

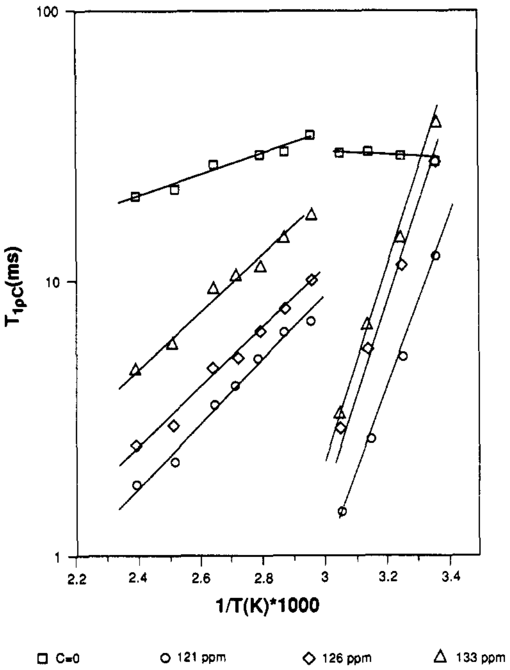

Figure 11. $\langle T_{1\rho C}\rangle$ temperature dependence for 30% small FP (F74B) in DMAc/LiCl.

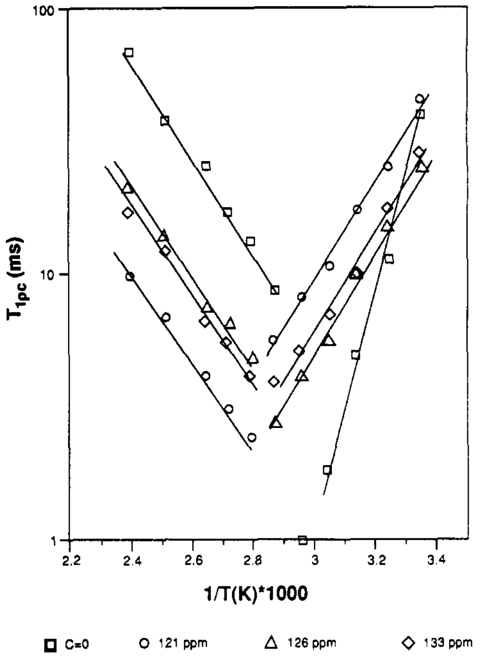

Figure 12. $\langle T_{1\rho C}\rangle$ temperature dependence for dry N74E, the network progeny of small FP (F74D).

The results for the swollen FP in Figure 11 are quite similar to those for swollen FP1. This is not surprising since the relaxation effects in the swollen network should be controlled primarily by the distance between branch points, which is the same in both FPs studied. Note the slightly higher activation energy for carbonyl relaxation at temperatures above the transition in FP2 versus FP1. We have insufficient data at this stage to directly assign the cause of this effect. It is possible that this is simply an effect of FP size, but a range of sizes would have to be studied to prove that.

Network 2. Sample N74E is the network progeny of FP2. Again we observe a transition in dry and swollen polymer; see Figures 12 and 13, but the relaxation behavior is quite interesting when compared with the FPs and network 1 results. The relaxation of the carbonyl carbon in the dry sample and that of the aromatic ring carbon with a resonance at 121 ppm in the swollen network do not behave as expected. We do not understand this behavior, and the results for these two carbon atoms are given only for the completeness of the data. In the dry network (Figure 12) we observe relatively high E_a for carbonyl and ring motions at low temperatures, with the carbonyl giving much more energetic motions. At temperatures above the transition the carbonyl and rings have essentially the same activation energy. This contrasts sharply with the results for the FPs and network 1 where the rings and carbonyls are decoupled at elevated temperatures.

The relaxation behavior in the swollen network (see Figure 13) also differs significantly from those of the FPs,

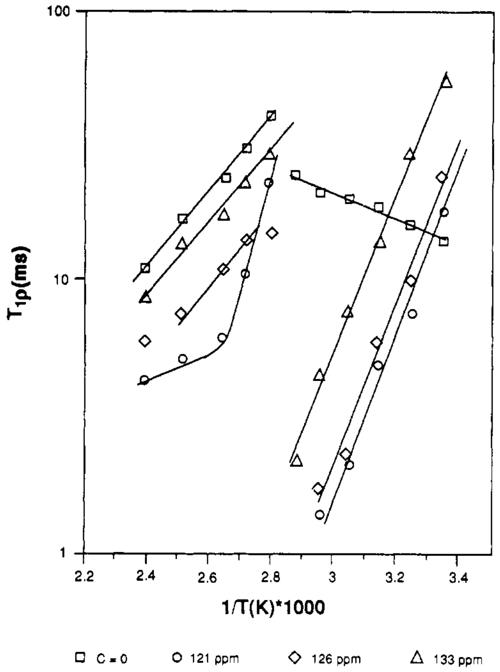

Figure 13. ⟨$T_{1\rho C}$⟩ temperature dependence for 30% N74E, the network progeny of small FP (F74D) in DMAc/LiCl.

network 1, and linear polymer. In particular, the behavior of the 121 ppm peak is different from that of the other aromatics. This is an aromatic protonated carbon, which is expected to behave in concert with the other ring carbons, as it does at temperatures below the transition. However, above the transition it shows a much higher activation energy than the other aromatics.

The other aromatics and carbonyl group are well behaved in the swollen network. The carbonyl and rings are decoupled at low temperature but show the same activation energy at elevated temperatures. This is the same behavior observed in the dry polymer. Above the transition, activation energies are significantly higher than in all the other samples but are still consistent with anti/syn and syn/anti interconversions. We know that networks made from small FPs have a much higher density of interpolymer covalent bonds, reflected by a very high shear modulus.[5] It may be that the higher activation energies observed for network N74E, especially above the transition temperature, are a reflection of the motional constraints imposed on the network segments by being a part of a more perfect "infinite" network of stiff segments and rigid branch points.

Conclusions

The solid-state ^{13}C NMR relaxation behavior of dry and DMAc/LiCl-swollen rigid aromatic polyamides was examined as a function of temperature. Highly branched stiff fractal polymers and their network progenies were studied together with their linear polyamide analogue for comparison. There is a strong solvent–polymer interaction with a possible fraction of crystallosolvates in all samples. Average spin–lattice relaxation rates in the rotating frame (⟨$T_{1\rho C}$⟩) are highly dependent on temperature in all polymers studied. A highly concentrated linear polyamide solution forms a liquid crystalline phase at 70 °C which persists to the maximum temperature studied, 150 °C. It becomes isotropic again on cooling. Transitions also occur in the branched FPs and their network progenies, but these do not exhibit liquid crystallinity.

Unlike the linear polyamide, the relaxations of the carbonyl carbons in the FPs and networks are decoupled from those of the ring carbons. The activation energies for the carbonyl carbons were calculated from Arrhenius plots and are consistent with relaxation through anti/syn and syn/anti interconversions of amide groups relative to the adjacent aromatic rings. Such interconversions were postulated previously as the mechanisms for bending of stiff polyamide segments in the network constrained from terminal movement at either or both ends. Interestingly, the activation energies for amide interconversion are expected to be identical with or very close to those associated with aromatic "ring flips" along the chain.

References and Notes

(1) Aharoni, S. M. *Macromolecules* **1982**, *15*, 1311.
(2) Aharoni, S. M., Wertz, D. H. *J. Macromol. Sci., Phys.* **1983**, *B22*, 129.
(3) Aharoni, S. M.; Edwards, S. F. *Macromolecules* **1989**, *22*, 3361.
(4) Aharoni, S. M.; Murthy, N. S.; Zero, K.; Edwards, S. F. *Macromolecules* **1990**, *23*, 2533.
(5) Aharoni, S. M. *Macromolecules* **1991**, *24*, 235.
(6) Aharoni, S. M.; Hatfield, G. R.; O'Brien, K. P. *Macromolecules* **1990**, *23*, 1330.
(7) Aharoni, S. M. *Macromolecules* **1988**, *21*, 185; and unpublished observations.
(8) Aharoni, S. M. *Macromolecules* **1987**, *20*, 2010.
(9) Aharoni, S. M. *Macromolecules* **1987**, *20*, 877; and unpublished observations.
(10) Aharoni, S. M. *Macromolecules* **1991**, *24*, 4286.
(11) Cholli, A. L.; Dumais, J. J.; Engel, A. K.; Jelinski, L. W. *Macromolecules* **1984**, *17*, 2399.
(12) English, A. D. *J. Polym. Sci.* **1986**, *B24*, 805.
(13) Jelinski, L. W.; Dumais, J. J.; Watnick, P. I.; Engel, A. K.; Sefcik, M. D. *Macromolecules* **1983**, *16*, 409.
(14) Bovey, F. A.; Jelinski, L. W. *J. Phys. Chem.* **1985**, *89*, 571.
(15) Fyfe, C. A. *Solid State NMR for Chemists*; CFC Press: Guelph, ON, Canada, 1983.
(16) Komororoski, R. A., Ed. *High Resolution NMR Spectroscopy of Synthetic Polymers in Bulk*; VCH Publishers: Deerfield Beach, FL, 1986.
(17) Stejskal, E. O.; Schaefer, J.; Sefcik, M. D.; McKay, R. A. *Macromolecules* **1981**, *14*, 275.
(18) Schaefer, J.; Sefcik, M. D.; Stejskal, E. O.; McKay, R. A. *Macromolecules* **1981**, *14*, 188.
(19) Schaefer, J.; Stejskal, E. O.; Steger, T. R.; Sefcik, M. D.; McKay, R. A. *Macromolecules* **1980**, *13*, 1121.
(20) Schaefer, J.; Stejskal, E. O.; Buchdahl, R. *Macromolecules* **1977**, *10*, 1121.
(21) Schaefer, J.; Sefcik, M. D.; Stejskal, E. O.; McKay, R. A. *Macromolecules* **1984**, *17*, 1479.
(22) Lyerla, J. R. In *High Resolution NMR Spectroscopy of Synthetic Polymers in Bulk*; Komororoski, R. A., Ed.; VCH Publishers: Deerfield Beach, FL, 1986.
(23) VanderHart, D. L.; Earl, W. L.; Garroway, A. N. *J. Magn. Reson.* **1981**, *44*, 361.
(24) VanderHart, D. L.; Garroway, A. N. *J. Chem. Phys.* **1979**, *71*, 2772.
(25) Frye, J. S.; Maciel, G. E. *J. Magn. Reson.* **1982**, *48*, 125.
(26) Stejskal, E. O.; Schaefer, J.; Waugh, J. S. *J. Magn. Reson.* **1977**, *28*, 105.
(27) Mehring, M. *Principles of High Resolution NMR in Solids*; Springer-Verlag: Berlin, Heidelberg, New York, 1983.
(28) Papkov, S. P.; Dibrova, A. K. *Polym. Sci. U.S.S.R.* (*Engl. Transl.*) **1979**, *20*, 2205.
(29) Iovleva, M. M.; Prozorova, G. Ye.; Smirnova, V. N.; Papkov, S. P. *Polym. Sci. U.S.S.R.* (*Engl. Transl.*) **1981**, *23*, 2278.
(30) Iovleva, M. M.; Smirnova, V. N.; Khanin, Z. S.; Volokhina, A. V.; Papkov, S. P. *Polym. Sci. U.S.S.R* (*Engl. Transl.*) **1981**, *23*, 2048.

Registry No. DMAc, 127-19-5.